

# Discharge Coefficients Through Perforated Plates

P. A. KOLODZIE, JR., and MATTHEW VAN WINKLE

University of Texas, Austin, Texas

The design variables that affect the pressure drop across dry perforated plates were determined and correlated. Average orifice coefficients were calculated for the perforated plates by using a modified form of the single-orifice flow equation.

The variables which affected the orifice coefficients were found to be the hole diameter, hole pitch, plate thickness, fraction of the plate covered by the perforated area, and a Reynolds number based on the hole diameter. The orifice coefficients have been correlated with these variables in dimensionless groupings.

The correlation presented covers a practicable range of variables for which the pressure drop may be predicted in design.

which affected the pressure drop across dry perforated plates.

## PREVIOUS INVESTIGATIONS

Some data on dry-perforated-plate pressure drop have already been reported by various authors (2, 4 to 8) in connection with other distillation studies. The results obtained by some of the investigators are plotted in Figure 1. Table 1 is a compilation

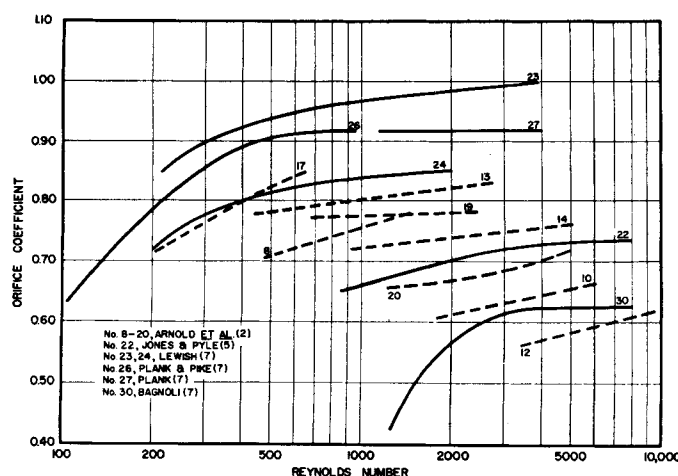


Fig. 1. Some results of previous investigators.

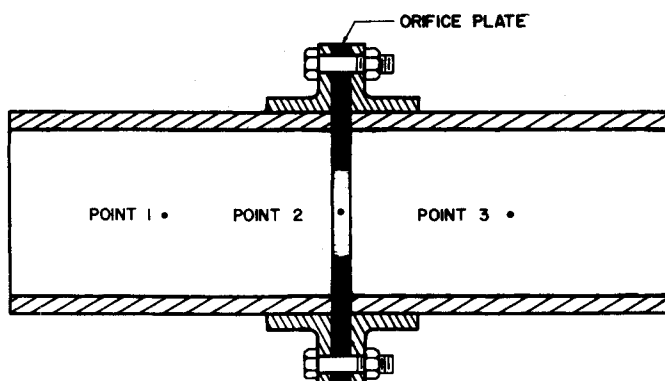


Fig. 2. Single-orifice plate in a circular conduit.

In the past few years there has been an increase in industrial use of perforated-plate distillation columns, as for many services the perforated-plate column has been found equivalent to, or better than, the generally used bubble-cap column. Since the perforated-plate column has come into general use only recently, however, there is still a lack of reliable design information.

One of the important design considerations in a distillation column is the pressure drop through the column. The major portion of the pressure drop is that through the plates. For design purposes the pressure drop across or through a plate has generally been considered to be a combination of two effects: (1) the pressure drop caused by the liquid head on the plate and (2) the pressure drop caused by the discharge of the vapor through the dry plate. This study was concerned with the second of these two effects. An investigation was undertaken to determine and correlate those variables

TABLE 1  
PLATE DATA OF PREVIOUS INVESTIGATORS

Plate	Investigator	Hole diam., in.	Free area, % column	T/d ratio	P/d ratio
1	8	0.125	0.7*	2.00	4.00†
2		0.1875	12.7*	1.33	2.67†
3		0.1875	3.2*	1.33	5.33†
4		0.1875	5.7*	1.33	4.00†
5		0.1875	5.7*	2.00	4.00†
6		0.1875	5.7*	0.67	4.00†
7		0.25	5.7*	1.00	4.00†
8	2	0.038	4.3	0.764	3.30†
9		0.059	3.9	0.492	3.70†
10		0.139	4.5	0.209	3.47†
11		0.250	4.5	0.115	3.48†
12		0.312	4.1	0.093	3.48†
13		0.083	10.5	0.350	3.27†
14		0.177	12.0	0.164	2.12†
15		0.235	11.9	0.123	2.12†
16		0.376	11.5	0.077	2.16†
17		0.039	18.5	0.743	1.62†
18		0.062	17.1	0.468	1.77†
19		0.144	17.8	0.201	1.74†
20		0.249	17.4	0.117	1.75†
21		0.309	16.2	0.094	1.82†
22	5	0.125	6.7	0.496	3.00†

P. A. Kolodzie, Jr., is at present with Humble Oil and Refining Company, Houston, Texas.

TABLE 1.—Continued  
PLATE DATA OF PREVIOUS INVESTIGATORS

Plate	Investigator	Hole diam., in.	Free area, % column	T/d ratio	P/d ratio
23	7 (Lewish)	0.039	21.8	0.570	2.04†
24		0.125	23.2	0.147	1.98†
25		0.033	4.82	0.498	4.33†
26	7 (Plank and Pike)	0.059	20.0	0.361	2.13†
27	7 (Plank)	0.059	20.0	0.361	2.13†
28	7 (Bagnoli)	0.125	1.22	—	7.50†
29		0.125	1.22	—	9.00†
30		0.125	2.24	—	6.00†
31	6	0.197	1.04	0.060	8.00†
32		0.197	4.59	0.060	4.00†
33		0.118	1.01	0.133	8.00†
34		0.118	4.51	0.133	4.00†
35		0.0787	1.30	0.200	8.00†
36		0.0787	4.70	0.200	4.00†
37		0.0393	1.24	0.400	8.00†
38		0.0393	4.64	0.400	3.00†
39		0.197	9.05	3.16	3.20†
40		0.0787	1.45	7.90	8.00†
41	4	0.125	18.8	1.00	2.00†
42		0.125	4.9	1.00	4.00†
43		0.250	5.4	1.00	4.00†
44		0.250	19.0	1.00	2.00†
45		0.500	4.9	1.00	4.00†
46		0.500	21.5	1.00	2.00†
47		0.375	5.1	1.00	4.00†
48		0.250	9.5	1.00	3.00†

\*Estimated.  
†Triangular.  
‡Square.

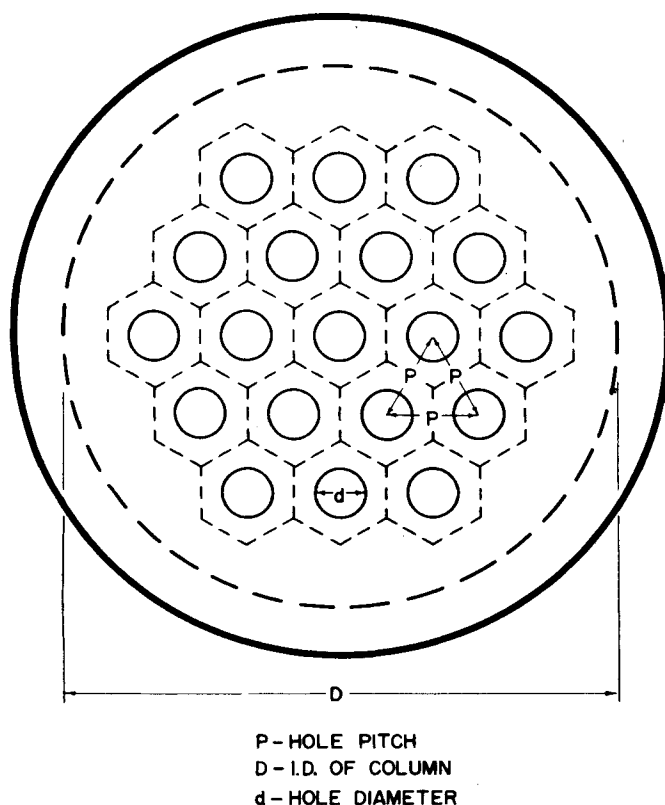


Fig. 3. A perforated plate with the holes on an equilateral-triangle pitch.

of the physical data for the perforated plates used by the various investigators. (Curves in Figure 1 correspond numerically to plate numbers in Table 1.)

Baines and Peterson (3) made a partial study of perforated barriers some years ago as part of an investigation on pressure drops across screens. They predicted that the discharge coefficients through the barriers were a function of a Reynolds number, solidity ratio, and perforation pattern.

Mayfield *et al.* (8) reported on one of the first investigations related to the design of perforated-plate columns. A study of dry-plate pressure drop was made on a 6-in.-diam. column using air. They concluded from their work that the discharge coefficients through the plates were independent of plate thickness, drilling pattern, and hole size. It was indicated that the coefficient did not vary with the Reynolds number over the ranges covered. Shortly after the appearance of the work of Mayfield *et al.* (8), Arnold *et al.* (2) reported a similar study using air in 6- and 15-in.-diam. columns. Arnold concluded that the discharge coefficients were a function of hole size, free area, and Reynolds number. These authors reported that an attempt at a correlation by use of a modified Reynolds number was unsuccessful and they proposed the following correlation:

$$P = kv^{1.8} \quad (1)$$

where  $k$ , a dimensional constant, was assumed to be dependent only on hole diameter and free area.

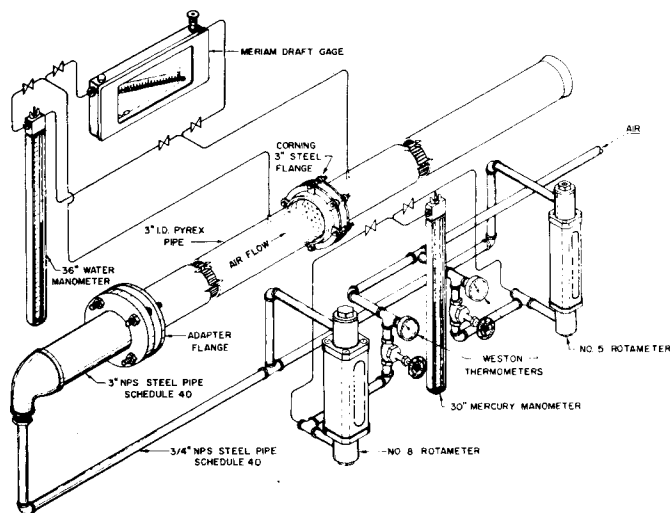


Fig. 4. General layout of the apparatus.

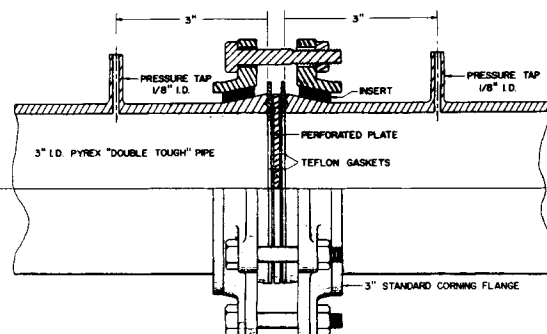


Fig. 5. Detail of pressure-tap and flange arrangement.

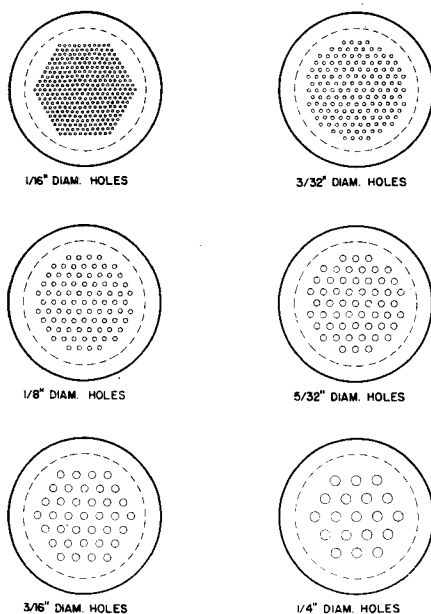


Fig. 6. Perforated-plate layouts for a pitch-to-hole-diameter ratio of 2.0.

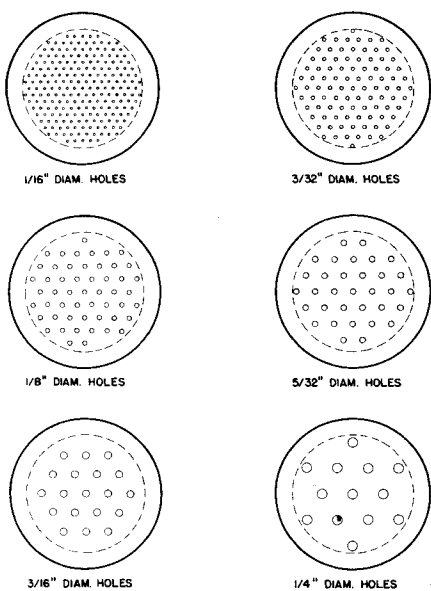


Fig. 7. Perforated-plate layouts for a pitch-to-hole-diameter ratio of 3.0.

Lewish (7), reported a study of the variables affecting pressure drop across perforated plates, using water in a 1.5-in.-diam. column. He also reported some work done by Bagnoli, Plank, and Plank and Pike. In general, Lewish verified the findings of Arnold and in addition concluded that a Reynolds number based on the perforation diameter was a definite correlating factor. The variable of plate thickness was not studied by Lewish. Kamei *et al.* (6) reported that discharge coefficients for dry perforated plates were a function of hole diameter and plate thickness only he tested a number of plates of different design using air in a 5.12-in.-diam. column.

Recently Hunt *et al.* (4) reported a study on a 6-in.-diam. column using air, Freon 12, carbon dioxide, argon, and methane. These authors proposed a dry-plate correlation based on the analogy between a plate perforation and a short tube with entrance and exit losses. Hunt *et al.* suggested that the discharge coefficients were probably

affected by the plate-thickness-to-hole diameter ratio. In their study, however this ratio was limited to 1.0.

#### THEORETICAL CONSIDERATIONS

The number and nature of the variables involved in a study of pressure drop

TABLE 2  
PHYSICAL DATA FOR PERFORATED PLATES

Hole diam., in.	$T/d$ ratio	No. holes	Free area, % column	Hole diam., in.	$T/d$ ratio	No. holes	Free area, % column
Hole pitch to hole diameter = 2.0				Hole pitch to hole diameter = 3.0			
0.0625	1.30	331	14.50	0.0625	1.30	207	9.08
0.0938	0.86	151	14.75	0.0938	0.86	93	9.08
0.125	0.65	85	14.75	0.125	0.65	52	9.03
0.1563	0.52	55	14.93	0.1563	0.52	33	8.96
0.1875	0.43	37	14.45	0.1875	0.43	19	7.42
0.250	0.33	19	13.20	0.250	0.33	13	9.03
0.0625	2.00	331	14.50	0.0625	2.00	207	9.08
0.0938	1.33	151	14.75	0.0938	1.33	93	9.08
0.125	1.00	91	15.80	0.125	1.00	52	9.03
0.125	1.00	85	14.75	0.125	1.00	37	6.42
0.125	1.00	61	10.60	0.125	1.00	31	5.38
0.125	1.00	37	6.42	0.125	1.00	19	3.30
0.1563	0.80	55	14.93	0.1563	0.80	33	8.96
0.1875	0.67	37	14.45	0.1875	0.67	19	7.42
0.250	0.50	19	13.20	0.250	0.50	13	9.03
0.0625	3.00	331	14.50	0.0625	3.00	207	9.08
0.0938	2.00	151	14.75	0.0938	2.00	93	9.08
0.125	1.50	85	14.75	0.125	1.50	52	9.03
0.1563	1.20	55	14.93	0.1563	1.20	33	8.96
0.1875	1.00	37	14.45	0.1875	1.00	19	7.42
0.250	0.75	19	13.20	0.250	0.75	13	9.03
0.0625	4.00	331	14.50	0.0625	4.00	207	9.08
0.0938	2.67	151	14.75	0.0938	2.67	93	9.08
0.125	2.00	85	14.75	0.125	2.00	52	9.03
0.1563	1.60	55	14.93	0.1563	1.60	33	8.96
0.1875	1.33	37	14.45	0.1875	1.33	19	7.42
0.250	1.00	19	13.20	0.250	1.00	13	9.03
Hole pitch to hole diameter = 4.0				Hole pitch to hole diameter = 5.0			
0.0625	1.30	121	5.31	0.0625	1.30	77	3.37
0.0938	0.86	55	5.37	0.0938	0.86	37	3.61
0.125	0.65	31	5.38	0.125	0.65	19	3.30
0.1563	0.52	19	5.17	0.1563	0.52	13	3.35
0.1875	0.43	13	5.07	0.1875	0.43	7	2.73
0.250	0.33	7	4.87	0.250	0.33	7	4.87
0.0625	2.00	121	5.31	0.0625	2.00	77	3.37
0.0938	1.33	55	5.37	0.0938	1.33	37	3.61
0.125	1.00	31	5.38	0.125	1.00	19	3.30
0.1563	0.80	19	5.17	0.1563	0.80	13	3.53
0.1875	0.67	13	5.07	0.1875	0.67	7	2.73
0.250	0.50	7	4.87	0.250	0.50	7	4.87
0.0625	3.00	121	5.31	0.0625	3.00	77	3.37
0.0938	2.00	55	5.37	0.0938	2.00	37	3.61
0.125	1.50	31	5.38	0.125	1.50	19	3.30
0.1563	1.20	19	5.17	0.1563	1.20	13	3.53
0.1875	1.00	13	5.07	0.1875	1.00	7	2.73
0.250	0.75	7	4.87	0.250	0.75	7	4.87
0.0625	4.00	121	5.31	0.0625	4.00	77	3.37
0.0938	2.67	55	5.37	0.0938	2.67	37	3.61
0.125	2.00	31	5.38	0.125	2.00	19	3.30
0.1563	1.60	19	5.17	0.1563	1.60	13	3.53
0.1875	1.33	13	5.07	0.1875	1.33	7	2.73
0.250	1.00	7	4.87	0.250	1.00	7	4.73

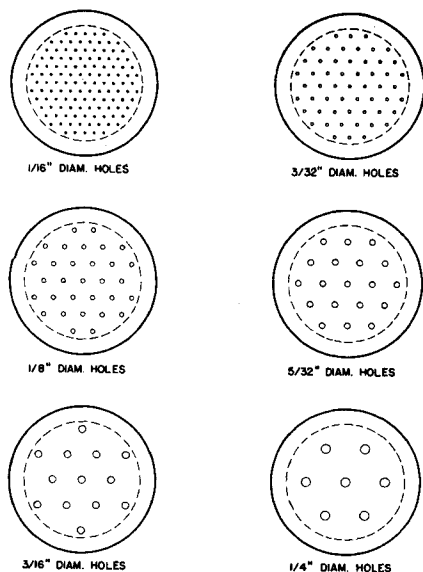


Fig. 8. Perforated-plate layouts for a pitch-to-hole-diameter ratio of 4.0.

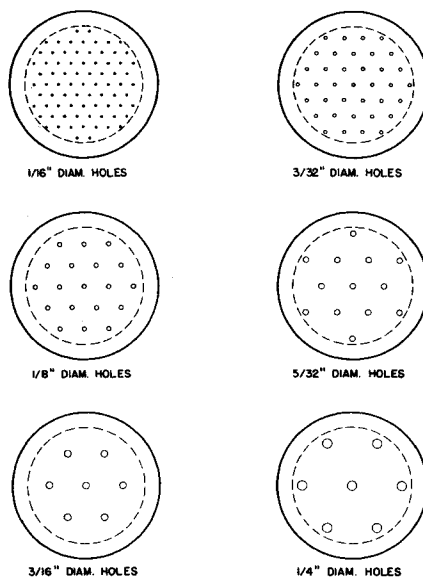


Fig. 9. Perforated-plate layouts for a pitch-to-hole-diameter ratio of 5.0.

across perforated plates make a rigorous theoretical analysis almost impossible. In this study a semiempirical approach was used. Discharge coefficients were calculated for the perforated plates and correlated against the physical characteristics of the fluid, column, and plate.

A typical perforated plate is shown in Figure 3. It was assumed to be composed of a number of individual orifices acting independently and in parallel. Although there is no theoretical basis for this assumption, it appears logical and allows

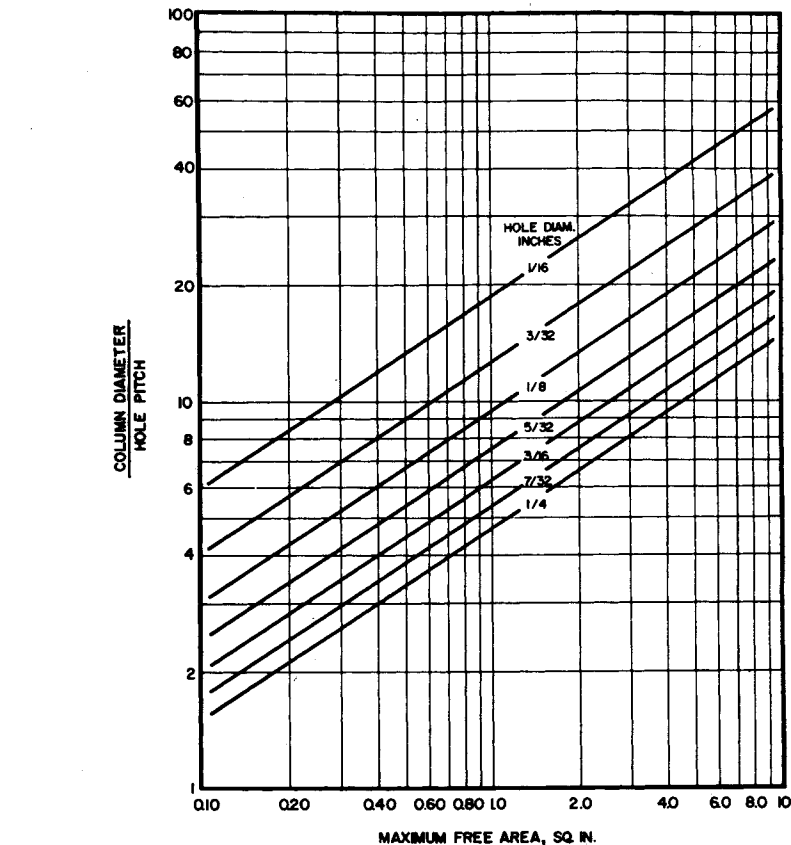


Fig. 10. Correlation for obtaining maximum free area for circular plates with holes on equilateral-triangular pitch.

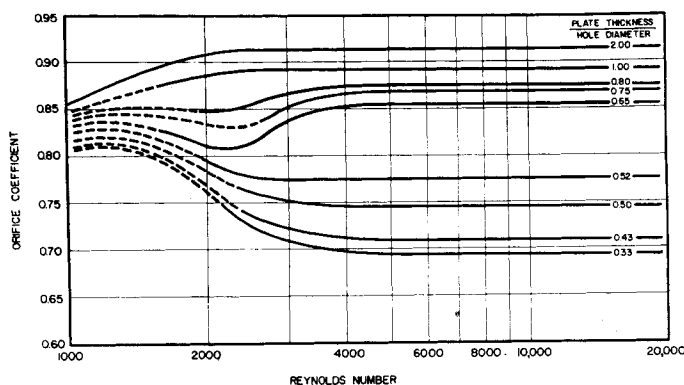


Fig. 11. Plot of orifice coefficient and Reynolds number for a pitch-to-hole-diameter ratio of 2.0.

the application, in part, of single-orifice relations. For a horizontal circular conduit containing a single circular orifice (Figure 2), a generally accepted flow equation for a compressible fluid is

$$v_2 = \frac{C}{Y} \sqrt{\frac{2g(-\Delta P_{1,3})}{\rho_1 \left[ 1 - \left( \frac{A_2}{A_1} \right)^2 \right]}} \quad (2)$$

For the perforated plate, it was assumed that the fluid flowing distributed equally among all holes. For this case the continuity equation can be written as

$$A_D v_D = (\text{No. holes}) (A_d) v = A_v v \quad (3)$$

where  $v_D$  = fluid velocity at  $A_D$   
 $v$  = fluid velocity at  $A_d$

Incorporating Equation (3) in the derivation of Equation (2) and altering the notation will give

$$v = \frac{C}{Y} \sqrt{\frac{2g(-\Delta P)}{\rho_D \left[ 1 - \left( \frac{A_f}{A_D} \right)^2 \right]}} \quad (4)$$

Equation (4) is the flow equation for perforated plates analogous to Equation (2) for single orifices.

A special A.S.M.E. report (1) has shown that the single-orifice coefficient can be correlated with the physical prop-

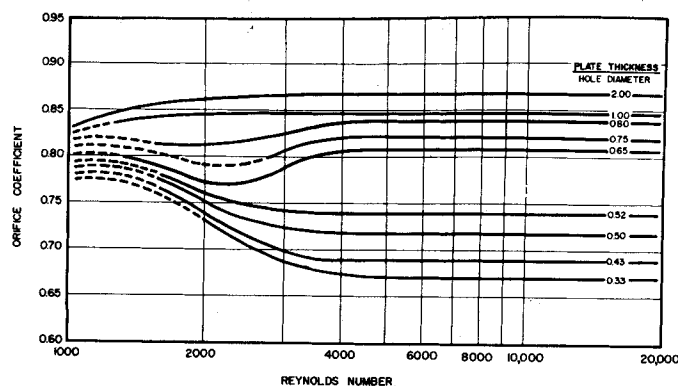


Fig. 12. Plot of orifice coefficient and Reynolds number for a pitch-to-hole-diameter ratio of 3.0.

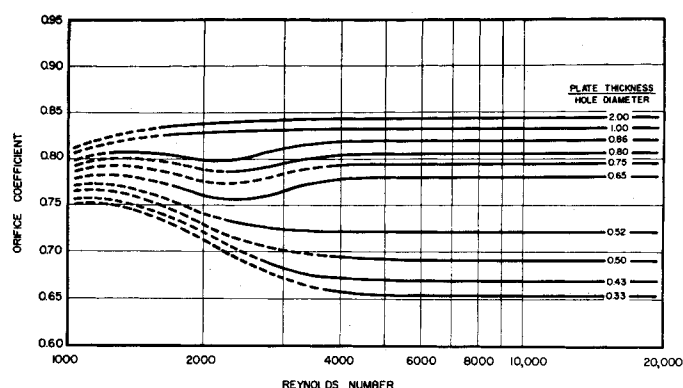


Fig. 13. Plot of orifice coefficient and Reynolds number for a pitch-to-hole-diameter ratio of 4.0.

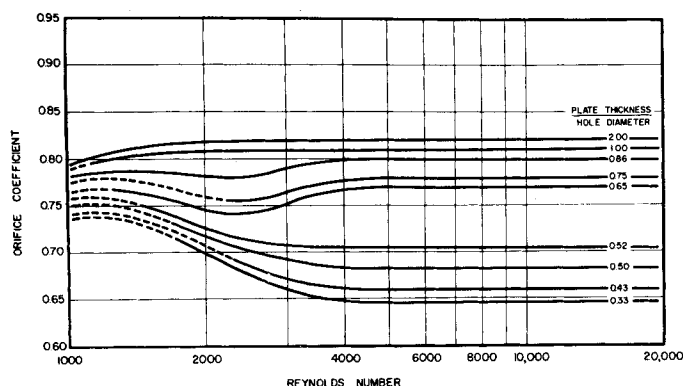


Fig. 14. Plot of orifice coefficient and Reynolds number for a pitch-to-hole-diameter ratio of 5.0.

erties of the conduit, fluid, and orifice plate through use of certain dimensionless groups. By dimensional analysis,

$$C = \mathfrak{F} \left[ \left( \frac{dvp}{\mu} \right), \left( \frac{d}{D} \right), \left( \frac{T}{d} \right) \right] \quad (5)$$

Though not included in the dimensional analysis, the coefficient has also been shown to be a function of pressure-tap location and shape of the upstream orifice edge.

Based on experimental work and the A.S.M.E. report (1), the variables that

were considered to affect the orifice coefficient for perforated plates were

1. Fluid velocity through the orifice  $v$
2. Fluid density  $\rho$
3. Fluid viscosity  $\mu$
4. Hole diameter  $d$
5. Hole pitch  $P$
6. Free area of plate  $A_f$
7. Maximum free area possible if total area of the plate were perforated  $A_t$
8. Thickness of the plate  $T$

Consideration of these variables in a dimensional analysis gave

$$C = \mathfrak{F} \left[ \left( \frac{dvp}{\mu} \right), \left( \frac{d}{P} \right), \left( \frac{T}{d} \right), \left( \frac{A_f}{A_t} \right) \right] \quad (6)$$

Pressure-tap location and shape of the upstream orifice edge were held constant in this investigation. The dimensionless groups in Equation (6) were used as the basis for correlating the experimental data.

## EXPERIMENTAL WORK

The experimental equipment (Figure 4) was designed specifically to measure pressure drop across perforated plates at known flow rates. Air, the only fluid used, was obtained from a 100 lb./sq. in. gauge system available in the laboratory. Two Fisher and Porter Flowrators (tube sizes 5 and 8) connected in parallel were used to measure the air flow rate. Depending on the flow range required one or the other flowrator was used. The temperature (Weston dial-type thermometer) and pressure (Meriam standard 30-in. mercury manometer) were measured at the entrance of each flowrator. The perforated plates were flanged between two sections of 3-in. I.D. Pyrex pipe. A 48-in. length of straight pipe was used as the upstream approach to the plate to avoid interference from upstream fittings (9). Pressure taps were located 3 in. upstream and 3 in. downstream from the plate. Details of the flange arrangement are shown in Figure 5. Pressure drops across the plates of less than 2 in. of water were measured with a Meriam draft gauge calibrated in 0.01-in. divisions. A Meriam standard 36-in. water manometer was used to measure pressure drops exceeding 2 in. of water.

A systematic method was used in making the plates so that a practical range of variables might be tested. Pitch-to-hole diameter ratios of 2.0, 3.0, 4.0 and 5.0 were selected with all plates being laid out on an equilateral-triangle pattern. Hole sizes of 1/16-, 3/32-, 1/8-, 5/32-, 3/16-, and 1/4-diam. were used. All holes were drilled on a vertical drill press with the plates backed by wooden blocks to prevent excess burring. After drilling, the plates were drawn across No. 0 emery paper on a flat surface to knock off the burrs. Thicknesses of the plates were 0.081, 0.125, 0.1875, and 0.25 in. Plates with 0.125-, 0.1875-, 0.25-in. thicknesses were made of red brass and the 0.081-in.-thick plates were made of yellow brass. All plates were 3.78 in. in diameter.

Combinations of all variables were used so that for each  $P/d$  ratio there were twenty-four different plates. Six additional plates were also used in a study of free-area effects. The physical data on the plates are listed in Table 2. Actual layout patterns for the plates are shown in Figures 6 to 9 and 20. In laying out the hole patterns on the plates, it was realized that the spread of holes over the plate would probably affect the orifice coefficient (shown later); therefore, the plates were laid out so that the holes covered a major portion of the plate. In this manner the effect of  $P/d$ , plate thickness, and hole diameter could be studied on the same basis.

The maximum number of holes that can be fully exposed on a circular plate depends upon the plate diameter and the hole pitch.

The free area will depend on the number and size of the holes used. A correlation relating plate diameter, hole pitch, and hole size to maximum free area is presented in Figure 10. The correlation was arrived at by simple geometric relations and will hold only for an equilateral-triangular hole pattern.

Several checks were made at the outset of the investigation to determine the degree of reproducibility which could be expected from the equipment and procedures used. Several runs were made independently on the same plate to check the consistency of the data. A comparison of the pressure drops yielded a maximum difference of only 3%. A check was also made to determine how closely the plates themselves could be reproduced. Identical plates were tested and a comparison of the pressure drops yielded a maximum difference of only 2%. It was concluded, therefore, that the methods used would produce plates which would give comparable results. Since the patterns on some of the plates were not symmetrical, it was necessary to determine the effect of the relative rotational position of the plates with respect to the pressure taps. No effect on pressure drop was found.

#### EXPERIMENTAL RESULTS

In the calculations involving the air flow, the ideal-gas law was used. The air was considered to be dry and to have a molecular weight of 29.0. Orifice coefficients were calculated from Equation (4) after certain simplifications had been introduced. Since the pressure drop did not exceed 15 in of water, an average air density of 0.0731 lb./cu. ft. (temperature = 95°F., pressure = 775 mm. Hg) was used. For the small pressure drops that were encountered, the expansion factor was found to be nearly unity (11). Incompressible flow was assumed. The average possible error was estimated to be about 2% for the calculated coefficients.

In following through with the dimensional analysis, a Reynolds number based on the hole diameter was calculated, an average viscosity for air (temperature = 95°F.) being obtained from Perry (10). For each  $P/d$  ratio, the orifice coefficient was plotted vs. the Reynolds number (Figures 11 to 14) for various parameters of  $T/d$  ratio. When all data points had been plotted, the curves became obliterated by the large number of overlapping points. To enhance the clarity of presentation the points were omitted from the figures. The curves presented represent the best average of the points (within 3% maximum deviation). In general, the Reynolds number covered a range from 2,000 to 20,000. The dashed lines in the figures represent extrapolation beyond the experimental data. These extrapolations were based on interpolation of the existing curves and the symmetry which existed for the various  $P/d$  groupings. Beyond a Reynolds number of 4,000 the coefficients became constant.

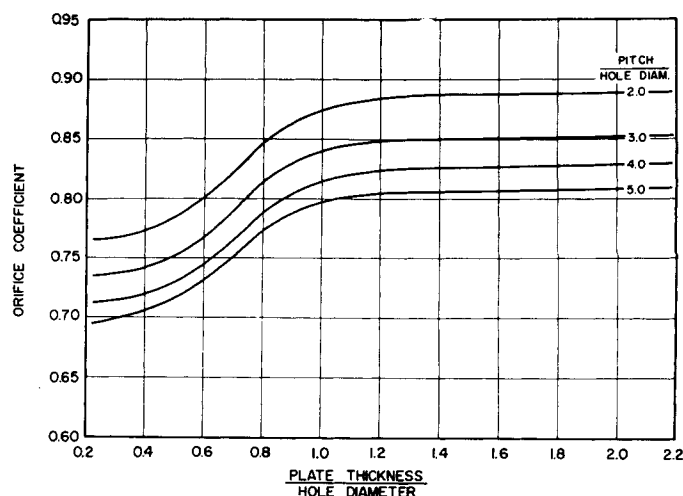


Fig. 15. Cross plot of Figures 11, 12, 13, and 14 at a Reynolds number of 2,000.

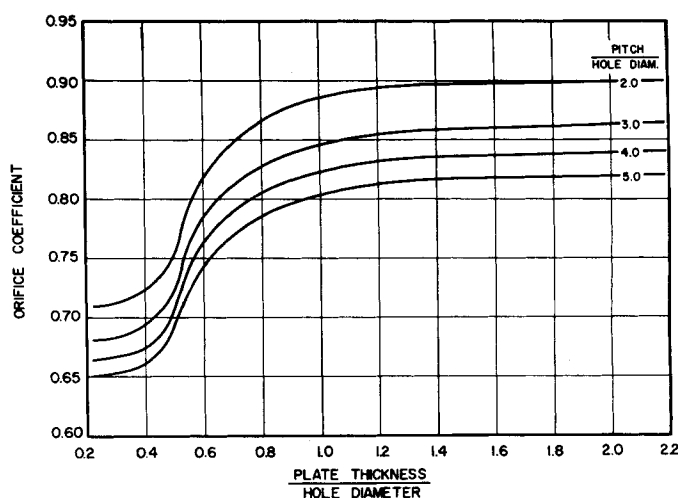


Fig. 16. Cross plot of Figures 11, 12, 13, and 14 at a Reynolds number of 3,000.

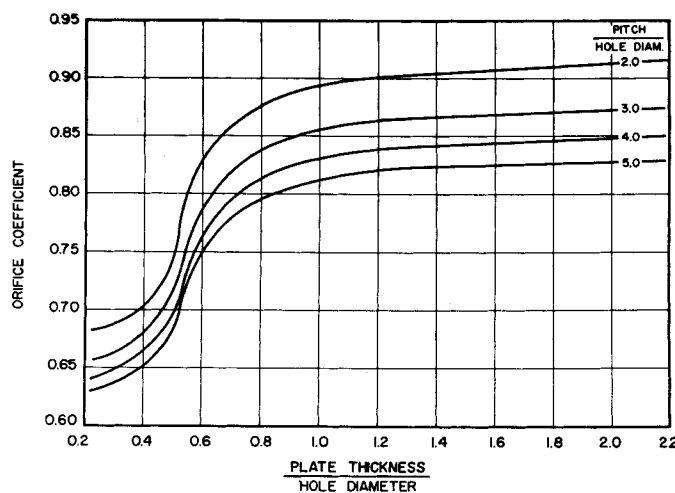


Fig. 17. Cross plot of Figures 11, 12, 13, and 14 at a Reynolds number of 10,000.

The general shape of the curves representing the smaller  $T/d$  ratios is similar to that of curves of the same type for the thin-plate ( $T/d < 0.125$ ) single orifice.

Cross plots were made from Figures 11, 12, 13, and 14 to determine the effect of the  $P/d$  ratio. The resulting plots were of coefficient vs.  $T/d$  ratio with the  $P/d$  ratio as parameter. Cross plots were

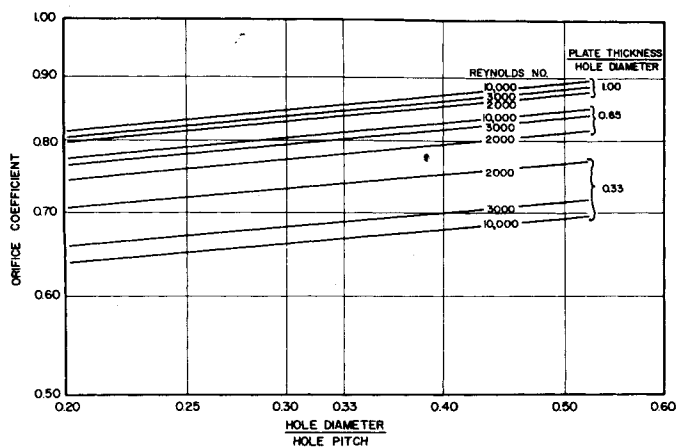


Fig. 18. Cross plots of Figures 15, 16, and 17 at various plate-thickness-to-hole-diameter ratios.

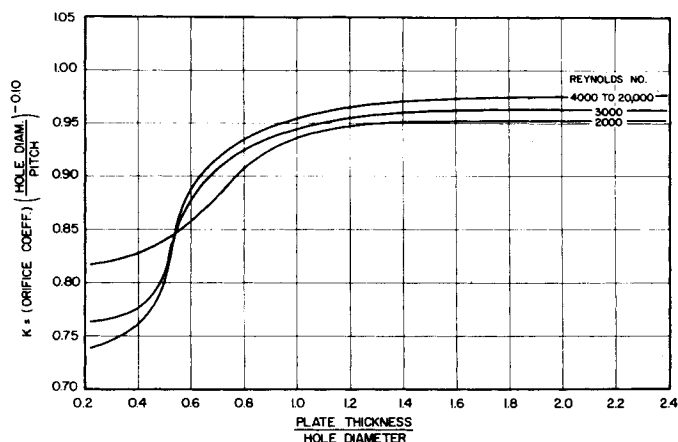


Fig. 19. A correlation relating orifice coefficient for perforated plates with the physical characteristics of the plate and gas.

taken at Reynolds numbers of 2,000, 3,000, and 10,000 (Figures 15 to 17). Since the coefficients are constant above Reynolds numbers of 4,000, Figure 17 will apply for a Reynolds number range from 4,000 to 20,000 and probably beyond.

Upon inspection of Figures 15, 16, and 17, a definite trend was noted between the curves of the different  $P/d$  ratios. A plot of coefficient vs. of  $d/P$  ratio on log-log paper revealed a series of straight parallel lines at the various  $T/d$  ratios (Figure 18). These curves can be expressed by the relation

$$\log C = \log K + \alpha \log \left( \frac{d}{P} \right) \quad (7)$$

where  $K$  = constant (function of  $T/d$ )

The family of curves can be represented by

$$C = K \left( \frac{d}{P} \right)^{0.10} \quad (8)$$

Equation (8) can be rearranged to

$$K = C \left( \frac{d}{P} \right)^{-0.10} \quad (9)$$

Since the value of  $K$  is constant for any  $T/d$  ratio, the curves in Figures 15, 16, and 17 may be represented as one curve by plotting  $K$  vs.  $T/d$  ratio. Figure 19 is a plot of  $K$  vs.  $T/d$  at Reynolds numbers of 2,000, 3,000, and 4,000 to 20,000.

The correlation presented in Figure 19 was derived by using perforated plates with holes covering a majority of the cross-sectional areas available. In distillation practice, however, chord weirs and downcomers limit the perforated area available. Perforated area is the area effectively covered with holes. In order to determine what effect the perforated area would have, several plates with different free-area patterns were tested. The layouts were chosen to simulate distillation-column plates (Figure 20). The physical characteristics of these plates are given in Table 2. The pressure drops for these plates were found to be independent of the rotational position of the pattern in relation to the pressure taps. Orifice coefficients for these plates were plotted against the Reynolds number with the free area as the resulting parameter (Figure 21).

The fraction of perforated area on the plates was expressed as a ratio of the

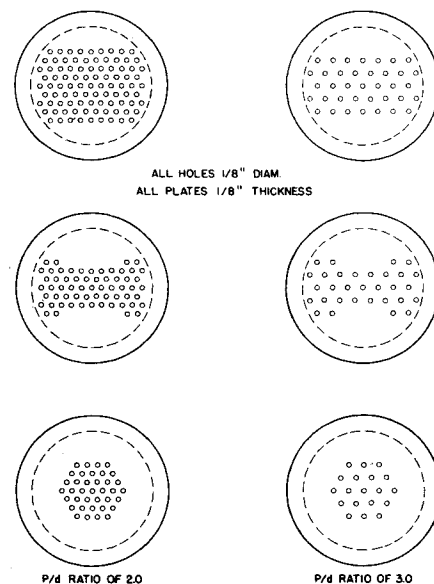


Fig. 20. Perforated-plate layouts for the free-area study.

actual free area ( $A_f$ ) to the maximum free area ( $A_t$ ) possible if the total area of the plate were perforated at the same  $P/d$  ratio and pattern. The maximum free area was determined from the correlation presented in Figure 10. At any given  $A_f/A_t$  ratio the  $A_f/A_D$  ratio is a function only of the  $P/d$  ratio. Figure 22 is a cross plot of Figure 21 at a Reynolds number 5,000. The coefficients were plotted vs.  $A_f/A_t$  ratio with the  $P/d$  ratio as the parameter. The dashed lines represent approximations based on a single data point. The curves shown are for a  $T/d$  ratio of 1.0, but they show the trends that can probably be expected at all  $T/d$  ratios. From Figure 22 it was concluded that the orifice coefficient is not affected by the distribution of the holes on a plate as long as the  $A_f/A_t$  ratio is greater than 0.60. Since the correlation in Figure 19 is based on  $A_f/A_t$  ratios of greater than 0.60, the correlation will apply between  $A_f/A_t$  ratios of 0.60 and 1.00. In actual practice the  $A_f/A_t$  ratio usually falls between 0.60 and 0.70.

#### APPLICATION OF CORRELATION

A generalized correlation is presented in Figure 19 which can be used for the design of perforated plates insofar as the dry-plate pressure drop is concerned. The correlation covers a wide range of practicable variables which are sufficient to cover most design needs. Although the correlation particularly applies to equilateral-triangular hole pattern, it may prove to be applicable to other arrangements.

The correlation presented was based only on air, the original supposition being that the Reynolds number is the criterion for dynamic similarity and

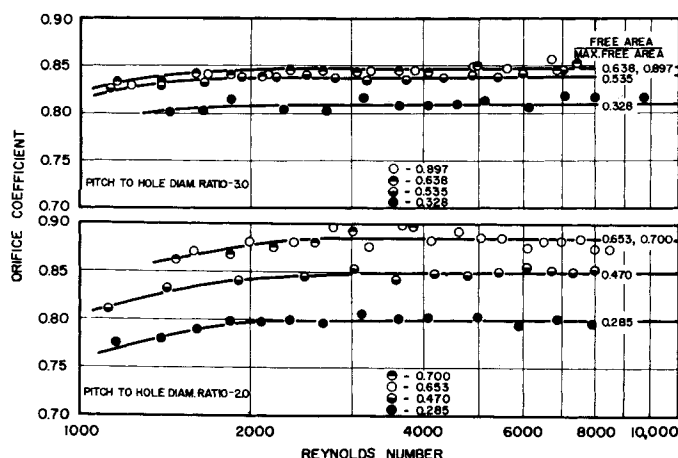


Fig. 21. Effect of free area on the orifice coefficient at a plate-thickness-to-hole-diameter ratio of 1.0.

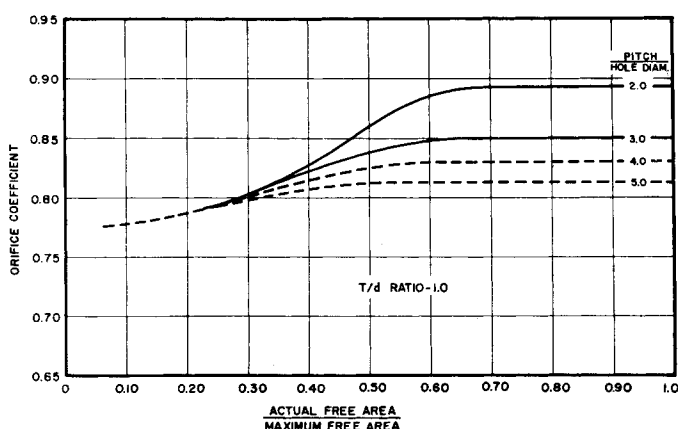


Fig. 22. Cross plot of Figure 21 at a Reynolds number of 5,000.

would generalize the correlation for other gases. Data presented by Hunt *et al.* (4) for air, carbon dioxide, methane, Freon 12, and argon were compared with values predicted from this correlation and found to have an average deviation of less than 5%. This seems to indicate that the correlation is applicable, in general, to other gases.

Although the correlation is based on data obtained from small-scale equipment, the dimensionless groups used in the correlation should allow application to larger columns. Scaling up of this type has been indicated by Mayfield *et al.* (8). Arnold *et al.* (2) also claim good agreement between 6 and 15-in.-diam. columns. A comparison was made between this correlation and the data presented by other investigators using larger columns. Data reported by Arnold *et al.* had an average deviation of less than 3%. Deviation from the data reported by Mayfield *et al.* was as high as 33% in one case, but generally the average was about 10%. Both Hunt and Mayfield used 6-in. columns and Arnold used 6- and 15-in. columns. With some reservations, it seems reasonable that the

correlation presented can be applied to larger diameter columns.

Certain generalizations can be made from the correlation about perforated-plate design. As a rule it is desirable to maintain a low dry-plate pressure drop across the plate. The following conditions were found to give the maximum coefficients: (1)  $T/d$  ratio of 1.0 or greater, (2)  $P/d$  ratio of 2.0 or less, and (3)  $A_f/A_t$  ratio from 0.60 to 1.00. For these conditions the optimum Reynolds-number range was found to be 4,000 to 20,000.

#### APPLICATION TO DESIGN OF COLUMNS

Although a Reynolds-number range from 2,000 to 20,000 has been covered in this work, the majority of commercial designs operate in a Reynolds-number range from 3,500 to 15,000. In this range the orifice coefficient becomes independent of Reynolds number and so the design engineer's use of these data is simplified.

It should be emphasized clearly that the data and correlations presented here were obtained from carefully finished plates and that commercially available

plates may not have the same characteristics. Comparisons of these data and those obtained from commercial types of perforations (2, 8) have been shown to be in good agreement.

#### NOTATION

- $A$  = cross-sectional area
- $A_f$  = free area of holes on a plate
- $A_t$  = maximum free area possible on a plate
- $C$  = average orifice coefficient
- $d$  = hole or orifice diameter
- $D$  = inside diameter of column or conduit
- $g$  = gravity constant
- $K$  = constant
- $P$  = hole pitch
- $\Delta P$  = pressure drop across a perforated plate
- $T$  = plate thickness
- $v$  = average fluid velocity in the orifice
- $Y$  = average expansion factor for the fluid
- $\alpha$  = slope of curves
- $\rho$  = fluid density in the orifice
- $\rho_D$  = fluid density at upstream pressure tap
- $\mu$  = fluid viscosity in the orifice

#### Subscripts

- $d$  = orifice or hole
- $D$  = column or conduit
- 1 = condition upstream from orifice
- 2 = condition in the orifice
- 3 = condition downstream from orifice

#### LITERATURE CITED

1. Am. Soc. Mech. Engrs. Special Committee on Fluid Meters, "Fluid Meters," Part I, New York (1937).
2. Arnold, D. S., C. A. Plank, and E. M. Schoenborn, *Chem. Eng. Progr.*, **48**, 633 (1952).
3. Baines, W. D., and E. G. Peterson, *Trans. Am. Soc. Mech. Engrs.*, **73**, 467 (1951).
4. Hunt, C. d'A., D. N. Hanson, and C. R. Wilke, *A.I.Ch.E. Journal*, **1**, 441 (1955).
5. Jones, J. B., and C. Pyle, *Chem. Eng. Progr.*, **51**, 424 (1955).
6. Kamei, S., T. Takamata, S. Mizuno, and Y. Tomizawa, *Chem. Eng. (Japan)*, **18**, No. 3, 108 (1954).
7. Lewish, W. T., *Prog. Report No. 7, Atomic Energy Comm.*, Microcard ORO 142 (1954).
8. Mayfield, F. D., W. L. Church, A. C. Green, D. C. Lee, and R. W. Rassmussen, *Ind. Eng. Chem.*, **44**, 2238 (1952).
9. Perry, J. H., ed., "Chemical Engineers' Handbook," 3 ed., p. 407, McGraw-Hill Book Company, Inc., New York (1950).
10. *Ibid.*, p. 371.
11. Stearns, R. F., R. J. Russell, R. M. Jackson, and C. A. Larson, "Flow Measurements with Orifice Meters," D. Van Nostrand Company, New York (1951).